AMERICAN SOCIETY FOR MICROBIOLOGY | Journal of Bacteriology®

RESEARCH ARTICLE

Sugar-Phosphate Toxicities Attenuate *Salmonella* Fitness in the Gut

Erin F. Boulanger,[a] Anice Sabag-Daigle,[a] Maryam Baniasad,[b] Katherine Kokkinias,[c] Andrew Schwieters,[d] Kelly C. Wrighton,[c] Vicki H. Wysocki,[b] Brian M. M. Ahmer[a]

[a]Department of Microbial Infection and Immunity, The Ohio State University, Columbus, Ohio, USA
[b]Department of Chemistry and Biochemistry, The Ohio State University, Columbus, Ohio, USA
[c]Department of Soil and Crop Science, Colorado State University, Ft. Collins, Colorado, USA
[d]Department of Microbiology, The Ohio State University, Columbus, Ohio, USA

ABSTRACT Pathogens are becoming resistant to antimicrobials at an increasing rate, and novel therapeutic strategies are needed. Using *Salmonella* as a model, we have investigated the induction of sugar-phosphate toxicity as a potential therapeutic modality. The approach entails providing a nutrient while blocking the catabolism of that nutrient, resulting in the accumulation of a toxic intermediate. We hypothesize that this build-up will decrease the fitness of the organism during infection given nutrient availability. We tested this hypothesis using mutants lacking one of seven genes whose mutation is expected to cause the accumulation of a toxic metabolic intermediate. The *araD*, *galE*, *rhaD*, *glpD*, *mtlD*, *manA*, and *galT* mutants were then provided the appropriate sugars, either *in vitro* or during gastrointestinal infection of mice. All but the *glpD* mutant had nutrient-dependent growth defects *in vitro*, suggestive of sugar-phosphate toxicity. During gastrointestinal infection of mice, five mutants had decreased fitness. Providing the appropriate nutrient in the animal's drinking water was required to cause fitness defects with the *rhaD* and *manA* mutants and to enhance the fitness defect of the *araD* mutant. The *galE* and *mtlD* mutants were severely attenuated regardless of the nutrient being provided in the drinking water. Homologs of *galE* are widespread among bacteria and in humans, rendering the specific targeting of bacterial pathogens difficult. However, the *araD*, *mtlD*, and *rhaD* genes are not present in humans, appear to be rare in most phyla of bacteria, and are common in several genera of *Enterobacteriaceae*, making the encoded enzymes potential narrow-spectrum therapeutic targets.

IMPORTANCE Bacterial pathogens are becoming increasingly resistant to antibiotics. There is an urgent need to identify novel drug targets and therapeutic strategies. In this work we have assembled and characterized a collection of mutations in our model pathogen, *Salmonella enterica*, that block a variety of sugar utilization pathways in such a way as to cause the accumulation of a toxic sugar-phosphate. Mutations in three genes, *rhaD*, *araD*, and *mtlD*, dramatically decrease the fitness of *Salmonella* in a mouse model of gastroenteritis, suggesting that RhaD, AraD, and MtlD may be good narrow-spectrum drug targets. The induction of sugar-phosphate toxicities may be a therapeutic strategy that is broadly relevant to other bacterial and fungal pathogens.

KEYWORDS *Salmonella*, gastroenteritis, colitis, narrow-spectrum antimicrobial, sugar-phosphate, sugar metabolism

Microbial pathogens are becoming increasingly resistant to antibiotics, which is a threat to global health and development. Strategies to overcome antibiotic resistance have been lacking as most classes of antibiotics were initially discovered more

Editor George O'Toole, Geisel School of Medicine at Dartmouth

Address correspondence to Brian M. M. Ahmer, ahmer.1@osu.edu.

The authors declare no conflict of interest.

For a commentary on this article, see https://doi.org/10.1128/JB.00411-22.

[This article was published on 16 November 2022 with an error in Fig. 2. Figure 2 was updated in the current version, posted on 1 December 2022.]

Received 10 September 2022
Accepted 21 October 2022
Published 16 November 2022

than 40 years ago, with a subsequent decline in the discovery rate (1). In 2017 the World Health Organization (WHO) published *Prioritization of Pathogens To Guide Discovery, Research and Development of New Antibiotics for Drug-Resistant Bacterial Infections, Including Tuberculosis*, recommending increased research efforts toward identification of novel antimicrobial targets in order to support the development of alternative classes of antibiotics (2). In this work, we explore the induction of sugar-phosphate toxicities as a novel therapeutic modality.

Sugar-phosphates are common intermediates of carbohydrate metabolic pathways (Fig. 1). These intermediates are quickly converted to the subsequent compound in the metabolic pathway by a downstream enzyme in that pathway. However, if that enzyme is inhibited, either by a small molecule or by mutation of the gene encoding it, the sugar-phosphate substrate of that enzyme will not be metabolized and will accumulate, thus leading to wide-ranging toxic effects (3). Consequently, the overall therapeutic strategy is to provide the sugar of interest to the organism while simultaneously inhibiting the appropriate enzyme in that sugar utilization pathway to induce toxic sugar-phosphate accumulation.

The 2017 WHO report recommended continued research and development strategies for novel antibiotics that target "common community bacteria," explicitly naming resistant *Salmonella* species and carbapenem-resistant *Enterobacteriaceae* (CRE) (2). In 2019 the CDC followed with its report on "Antibiotic Resistance Threats in the United States," considering the CRE an "urgent" priority and the fluoroquinolone-resistant nontyphoidal *Salmonella* serovars "serious" priorities (4). *Salmonella enterica* is a Gram-negative, facultative anaerobe that encompasses over 2,500 serovars, many of which cause diseases ranging from self-limiting gastroenteritis to systemic typhoid fever (5, 6). *Salmonella enterica* is among the top causes of hospitalization and death by foodborne pathogens in the United States and globally (7–9). Symptoms of nontyphoidal *Salmonella* infection include an inflammatory diarrhea with acute abdominal pain, sometimes with a fever lasting up to a week. Though most cases are self-limiting, more complicated cases can cause bloodstream infections, especially in young children (under 5 years old), the elderly, and the immunocompromised, and these require therapeutic intervention. Oddly, for the vast majority of uncomplicated infections that remain within the intestinal tract, antibiotics are often ineffective or can even worsen symptoms or prolong *Salmonella* shedding (10–15). This outcome may be because broad-spectrum antibiotics eliminate the colonization resistance provided by the normal microbiota. Such an idea aligns with the pathogenesis of *Salmonella*, as disruption of the microbiota is of critical importance to *Salmonella* infection. To disrupt the microbiota, *Salmonella* uses a pair of type III secretion systems (T3SSs) to promote the invasion of epithelial cells and to provoke a strong inflammatory response (16–21). The inflammatory response disrupts the normal microbiota and causes nutrients and respiratory electron acceptors to accumulate (22–27). *Salmonella* then thrives on these nutrients, becoming greater than 50% of the gut microbial population (22, 28, 29). In contrast to broad-spectrum antibiotics, a narrow-spectrum therapeutic that exclusively targets *Salmonella* in the gastrointestinal tract without disrupting the normal microbiota could potentially alleviate the symptoms and shorten the duration of uncomplicated infections as well as reduce the number of infections that progress to the bloodstream.

In this work, we assembled a collection of mutations in seven genes that we hypothesized would cause a sugar-phosphate toxicity and characterized these mutants *in vitro* and in a mouse model of *Salmonella*-mediated gastroenteritis. Our findings suggest that the mannitol, rhamnose, and arabinose utilization pathways each contain an enzyme (MtlD, RhaD, and AraD, respectively) that could be inhibited to induce a potent sugar-phosphate toxicity that dramatically attenuates the fitness of *Salmonella* within the mouse gastrointestinal tract. We then used a bioinformatics approach to determine that these three enzymes would likely provide narrow-spectrum targets for

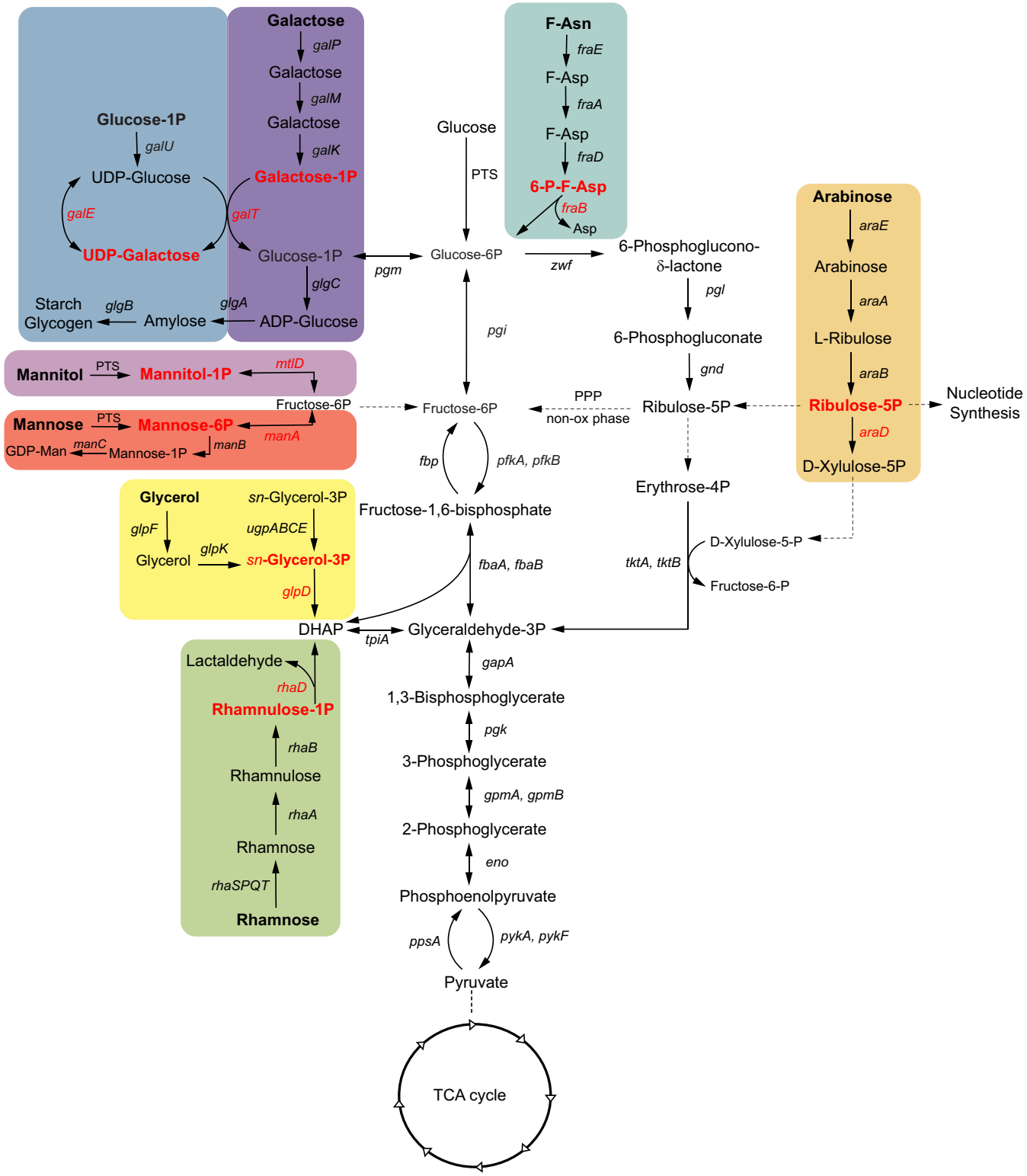

FIG 1 Metabolic pathways of selected carbohydrates. Each sugar utilization pathway is highlighted with a different color. The genes encoding the enzymes that cause sugar-phosphate accumulation when mutated, and the sugar-phosphates, are in red. TCA, tricarboxylic acid. This figure was adapted from reference 3.

the *Enterobacteriaceae*, as they are not present in humans and are uncommon among other bacteria.

RESULTS

Identification and mutation of genes predicted to cause sugar-phosphate toxicity in *Salmonella*. Throughout this work we use genetic mutations to eliminate the activity of the targeted enzymes. This strategy serves as a proxy for small-molecule inhibitors of those enzymes that would be used in real-world therapeutic applications. Most genes within a given sugar utilization pathway are required for utilization of only that sugar, rendering those mutants unable to grow if the sugar of interest is the sole nutrient source (i.e., a *galK* mutant is galactose negative). We will refer to these as sugar utilization genes. The genes that give rise to sugar-phosphate toxicity when mutated are both negative and sensitive. Such mutants are unable to grow on other nutrients when the sugar of interest is present due to the sugar-phosphate accumulation causing toxicity (i.e., a *galE* mutant is both galactose negative and galactose sensitive). For brevity, we refer to these as sugar-phosphate genes. Also for simplicity, we are referring to all of the phosphorylated metabolic intermediates in this work as sugar-phosphates, although glyercol-3-P (Gly-3P) and mannitol-1-P (Mtl-1P) are polyol-phosphates, and 6-phosphofructose-aspartate (6-P-F-Asp) is a phosphorylated Amadori product.

We recently reviewed the topic of sugar-phosphate toxicities (3). From that information, we assembled a list of 14 genes of *Salmonella* either that are known, or that we hypothesize, to cause a sugar-phosphate toxicity when mutated and assuming the appropriate sugar is provided (*fraB*, *araD*, *galE*, *galT*, *otsB*, *pgi*, *pfkA*, *pfkB*, *rhaD*, *sgrS*, *fbaB*, *glpD*, *mtlD*, and *manA*). Six of these are involved with glucose metabolism and are not discussed further, except for being included in phylogenetic analyses below. Another is *fraB*, which we have characterized extensively in the past and include here only for comparison (30–34). The remaining seven are characterized in this work (*araD*, *galE*, *galT*, *rhaD*, *glpD*, *mtlD*, and *manA*) (Fig. 1 and 2). Mutations in these seven genes were moved from the collection of Andrews-Polymenis and McClelland (available at BEI Resources) into our wild-type strain using phage P22 transduction. Typically, two types of mutations are available, an insertion of either a chloramphenicol (Cam^r) or a kanamycin (Kan^r) resistance gene into a deleted target gene. After moving these mutations into our laboratory strain, we then removed the antibiotic resistance gene using Flp recombinase, leaving a deletion and scar. Therefore, we have a Cam^r insertion, a Kan^r insertion, and a deletion for each of the seven genes of interest, with the exceptions being that we are lacking an *araD* deletion mutant and a *manA*::Kan insertion mutant.

The induction of sugar-phosphate toxicities in *Salmonella* leads to growth inhibition. Mutants predicted to suffer sugar-phosphate toxicity were grown in three types of media: (i) nutrient-rich lysogeny broth (LB), plus or minus the sugar of interest; (ii) M9 minimal medium with fructose, plus or minus the sugar of interest; and (iii) M9 containing only the sugar of interest (no additional carbon source). D-Galactose was used as the sugar of interest with the *galE* and *galT* mutants, L-rhamnose with the *rhaD* mutants, glycerol with *glpD* mutants, D-mannitol with *mtlD* mutants, D-mannose with *manA* mutants, and L-arabinose with *araD* mutants. As expected, each mutant grew normally in LB or M9 fructose if the sugar of interest was absent. However, they failed to grow if the sugar of interest was the only carbon source present, i.e., they were all sugar negative (Fig. 2). The addition of the sugar of interest to these media resulted in no growth defect for the *glpD* mutant and a modest growth defect for the *manA* mutant that occurred only in M9 medium and not in LB. On the other hand, the *galE*, *galT*, *mtlD*, and *rhaD* deletion mutants had substantial growth defects in both growth media. While we do not have a deletion mutant of *araD*, both the Cam^r and Kan^r insertion mutants of *araD* had severe growth defects.

With some genes, different results are obtained with different mutations. Specifically, the Cam^r insertion mutations in the *galE* and *galT* genes do not confer growth defects in

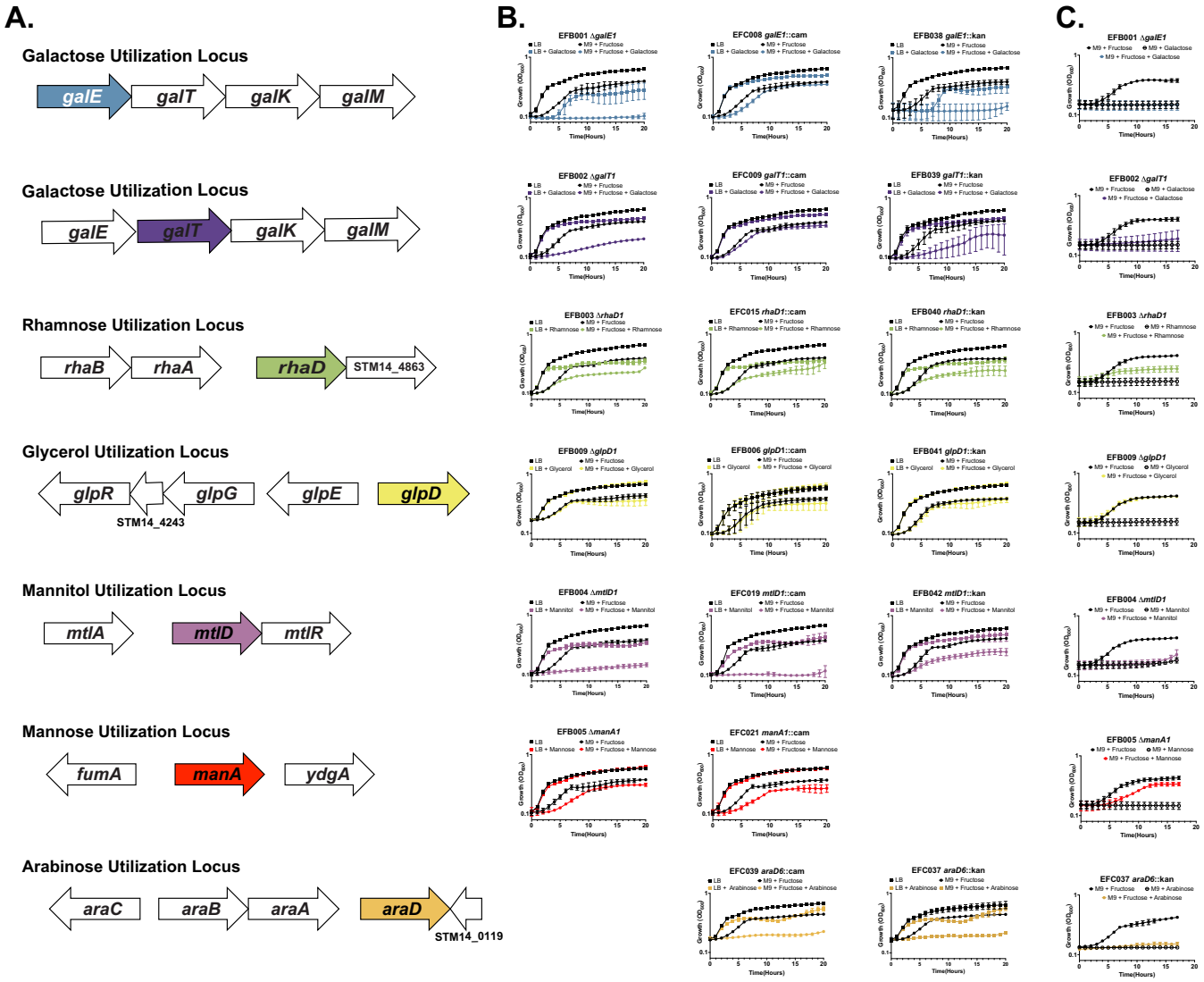

FIG 2 Sugar-phosphate toxicity causes inhibition of growth of *Salmonella* mutants. (A) Genetic organization of sugar utilization loci in *Salmonella enterica* strain ATCC 14028. The genes predicted to cause sugar-phosphate toxicity when mutated are in color. (B) Cultures grown overnight in LB were washed and subcultured 1:100 into LB or M9 plus fructose (5 mM), with or without the indicated sugar at 5 mM. (C) Cultures grown overnight in LB were washed and subcultured 1:100 into M9 plus fructose (5 mM), with or without the indicated sugar at 5 mM, or M9 plus the indicated sugar as the only carbon and energy source. Growth was measured by OD_{600} readings every hour for 17 to 20 h. Error bars represent the standard deviation from two independent experiments performed in duplicate ($n = 4$).

the presence of galactose. The Cam^r insertions in the BEI Resources mutant collection are oriented opposite the gene being mutated and are polar. The *galE* and *galT* genes are contained within the same operon, and the Cam^r insertions are likely to disrupt expression of the downstream gene, *galK* (Fig. 2). In the absence of *galK*, galactose cannot be phosphorylated and so toxic intermediates do not accumulate in the *galE* and *galT* mutants. The Kan^r insertions in the BEI Resources mutant collection are in the opposite orientation from the Cam^r insertions, have no transcription terminator, and are not polar. Thus, in some cases downstream genes may be expressed at higher-than-wild-type levels due to the promoter of the Kan^r gene. We were unable to obtain a deletion mutant of *araD*. Fortunately, *araD* lies at the end of an operon, and so polarity should not be an issue. Indeed, the *araD*::Cam and *araD*::Kan insertions yield similar results in growth curves with both being inhibited by the presence of arabinose (Fig. 2). Interestingly, the *mtlD*::Cam mutant has a more severe growth defect than either the *mtlD*::Kan or *mtlD* deletion mutant. This defect is likely due to polarity on *mtlR*, a repressor of mannitol utilization (Fig. 2). In the absence of the repressor, the mannitol

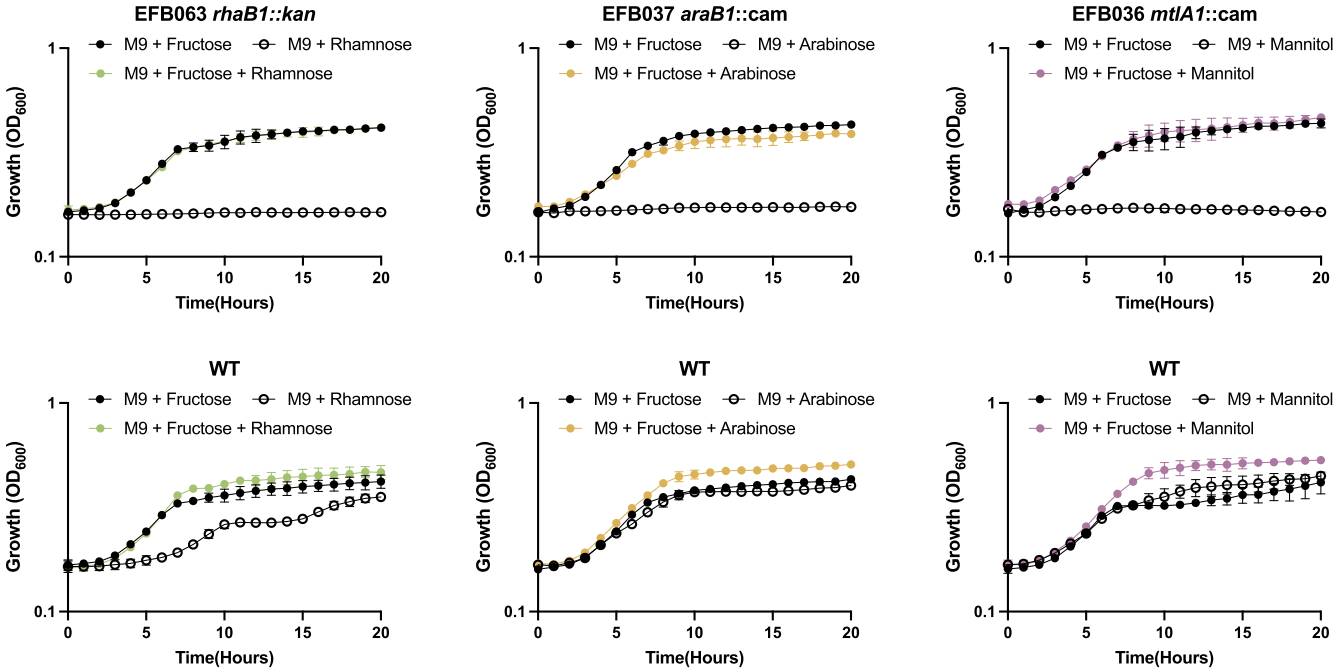

FIG 3 Sugar utilization mutants do not experience toxicity and are unable to use the sugar of interest as a sole nutrient source. These sugar utilization mutants are those containing mutations in a gene whose enzyme functions upstream of the toxic sugar-phosphate in that pathway. Cultures grown overnight of the indicated mutants and wild type (WT) were washed and subcultured 1:100 into M9 containing fructose (5 mM), the indicated sugar only (5 mM), or both fructose and the indicated sugar (5 mM each). Growth was measured with OD_{600} readings every hour for 20 h. The WT is strain 14028. Error bars represent the standard deviation from one experiment performed in triplicate (n = 3).

phosphotransferase system (PTS) transporter, encoded by *mtlA*, may have abnormally high expression, leading to increased concentrations of Mtl-1P. We do not suspect that polarity has an impact on the toxicity phenotypes observed with the *rhaD* mutants, as *rhaD* lies at the end of an operon and all three mutations confer the same phenotype (Fig. 2).

In contrast to the sugar-phosphate genes, most of the other genes in sugar utilization pathways cause only an inability to utilize a particular sugar when mutated. Such mutants are not intoxicated by the presence of that sugar (i.e., they are sugar negative, not sugar sensitive). We demonstrate this phenotype using a *rhaB*, *mtlA*, and *araB* mutant. These mutants are unable to use rhamnose, mannitol, or arabinose, respectively, but grow like the wild type in the presence of each sugar as long as another carbon and energy source is available (fructose in this case) (Fig. 3).

Measurement of sugar-phosphate accumulation. To test the hypothesis that phosphorylated metabolic intermediates are indeed accumulating in these mutants, we performed targeted metabolomics using mass spectrometry (MS) on cell extracts of select sugar-phosphate mutants compared to wild-type controls grown under the same condition. In order to use a quantitative approach, standards of each sugar-phosphate being measured were required to determine the metabolite's mass-over-charge ratio and the best transition state for quantitation and to build a standard curve. For this reason, we were limited by the commercial availability of compounds and thus examined only a subset. Mutants and wild-type controls were grown in LB supplemented with the appropriate sugar for 4 h, at which point cell pellets were harvested, metabolites were extracted, and liquid chromatographic-mass spectrometric analysis was performed. The results were normalized to total protein concentration. In this experiment, we found that mutants which exhibit growth defects do in fact accumulate the predicted sugar-phosphate compared to their wild-type controls (Fig. 4). More specifically, we find that the *mtlD* and *araD* mutants accumulate Mtl-1P and ribulose-5-phosphate (Ru-5P), respectively, compared to wild-type cells in which the sugar-phosphate concentrations are below the limit of detection. Additionally, as expected from

A.

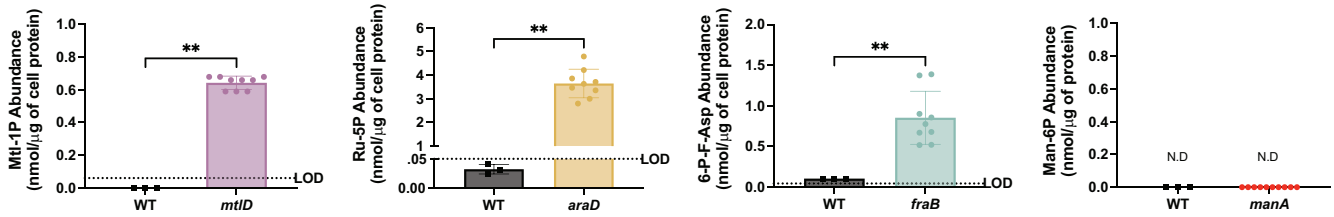

B.

Compound	Q1 (m/z)	Q2 (V)	Q3 (m/z)
6-P-F-Asp	376	15	242
Ru-5P	253	20	173
Mtl-1P	269	17	189
Man-6P	283	20	185
[^{13}C]-F-Asn	301	13	283

FIG 4 Quantitation of sugar-phosphate accumulation in selected mutants. (A) Liquid chromatographic-mass spectrometric (LC-MS) measurements in wild-type (WT) and mutant cells based on one transition for mannitol-1-phosphate (Mtl-1P), ribulose-5-phosphate (Ru-5P), 6-phosphofructose-aspartate (6-P-F-Asp), and mannose-6-phosphate (Man-6P) and normalized to protein concentration. A unique transition was selected for each sugar-phosphate from the table in panel B. (B) Transitions. The transition *m/z* 301→283 of [^{13}C]F-Asn with a collision energy of 13 eV was used for normalization. Skyline (v20.2; MacCoss Lab, Department of Genome Sciences, University of Washington, Seattle, WA, USA) was used for calculating the peak area of transition. The *mtlD* mutant is EFC019 (*mtlD1*::Cam), the *araD* mutant is EFC037 (*araD6*::Cam), the *fraB* mutant is HMB206 (*fraB80*::Kan), and the *manA* mutant is EFC021 (*manA1*::Cam). Each mutant was grown in LB containing a 5 mM concentration of the corresponding sugar for 4 h. LOD, limit of detection; N.D., not detected. $n = 3$ biological replicates with 3 technical replicates and 1 biological replicate with 3 technical replicates for WT. Statistical significance between groups was calculated using a two-tailed Mann-Whitney test (**, $P < 0.01$).

previous work we observed the accumulation of 6-phosphofructose-aspartate (6-P-F-Asp) in a *fraB* mutant (30). In contrast, the *manA* mutant, which does not have a growth defect in the presence of mannose in LB, predictably does not have a detectable accumulation of mannose-6-P (Man-6P).

Sugar-phosphate toxicity attenuates the fitness of *Salmonella* in a mouse model of infection. Since sugar-phosphate toxicity inhibits the growth of *Salmonella in vitro*, we tested the hypothesis that these same mutants would be attenuated during infection of the murine gastrointestinal tract. We employed a competition style of experiment with a streptomycin-treated Swiss Webster mouse model (30). In this model, mice are treated with streptomycin 24 h prior to infection in order to disrupt the normal microbiota and promote *Salmonella* colonization (35). For infection, the inoculum is prepared as a 1:1 ratio of wild type and a mutant and is delivered via oral gavage at a dose of 1×10^7 CFU. For these experiments, we used strains in which the gene of interest was deleted, and a kanamycin resistance gene was present in a separate, neutral location downstream of *pagC* (except for the *araD* mutant, which contained the kanamycin resistance gene within the *araD* gene) (32, 36). The wild-type strain was marked with a chloramphenicol resistance gene, in the same neutral location downstream of *pagC*, so that we could distinguish between wild type and mutant using selective medium. Because it was unclear at the start of these experiments which sugars, if any, would be available to *Salmonella* in the murine gastrointestinal tract, we performed the experiments with or without exogenous sugar (100 mM) provided in the animal's drinking water. At 4 days postinfection, the mice were euthanized, and each cecum was harvested, homogenized, and dilution plated on selective medium to enumerate recovered CFU for the two different strains (Fig. 5).

The *araD* mutant was modestly attenuated in the absence of arabinose in the water and severely attenuated in its presence. The *galE* and *mtlD* mutants were both severely

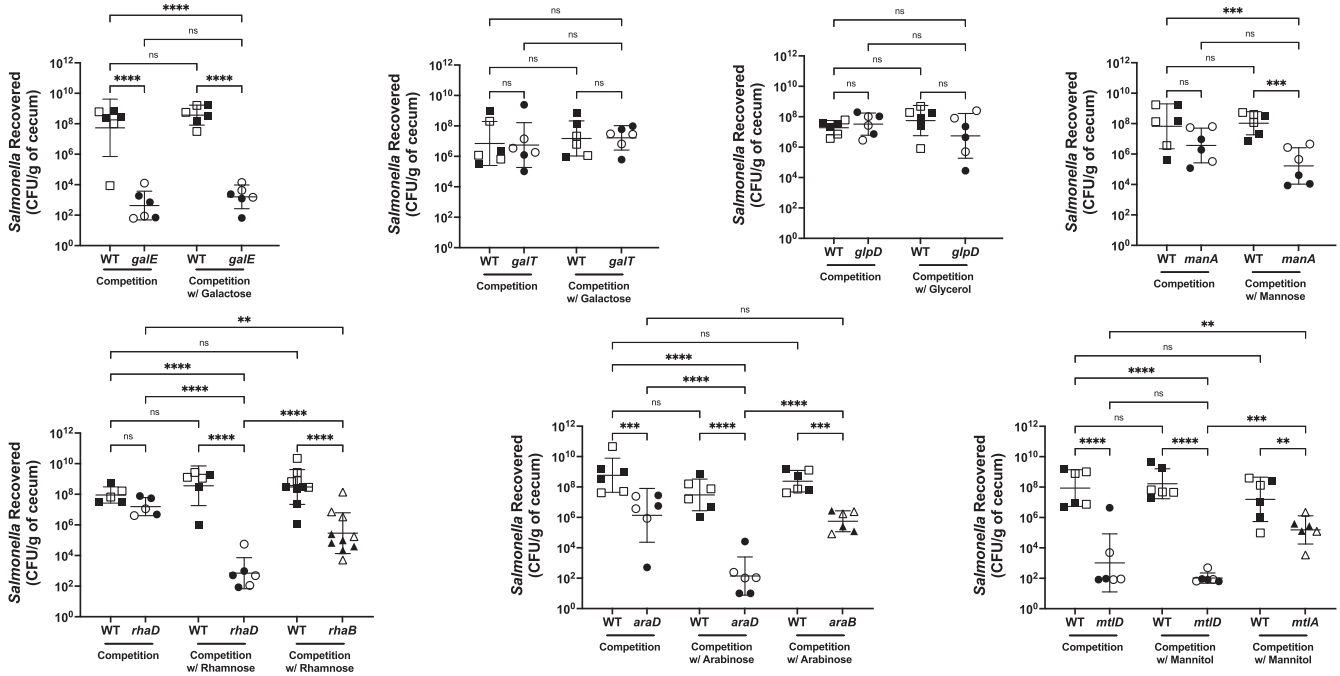

FIG 5 Sugar-phosphate toxicity causes attenuation of *Salmonella* in a mouse model of infection. Competition experiments between wild-type (WT) and mutant bacteria were performed in streptomycin-treated Swiss Webster mice. A 1:1 mixture of WT and the indicated mutant (1×10^7 CFU each) was administered orally to Swiss Webster mice that had been treated 24 h earlier with 20 mg of streptomycin. Where indicated, mice were provided sugar (100 mM) in their drinking water. At 4 days postinfection, mice were euthanized and ceca were harvested for enumeration of CFU. Statistical significance of differences between groups was determined using one-way analysis of variance with noncorrected multiple comparisons (*, P value < 0.05; **, P value < 0.005; ***, P value < 0.0005; ****, P value < 0.00005; ns, not significant). Filled and open symbols indicate male and female mice, respectively. The *galE* mutant is EFB053, the *galT* mutant is EFB054, the *glpD* mutant is EFB056, the *manA* mutant is EFB058, the *rhaD* mutant is EFB055, the *rhaB* mutant is EFB063, the *araD* mutant is EFC039, the *araB* mutant is EFB037, the *mtlD* mutant is EFB057, and the *mtlA* mutant is EFB036. The WT strain for every competition except those with *araB* and *mtlA* is JLD1214. The WT strain used for competitions with *araB* and *mtlA* is EFB051.

attenuated with and without sugar in the water. In all three cases, the attenuation observed in the absence of sugar in the drinking water suggests either that sugar was available to *Salmonella* in the gastrointestinal tract or that these mutants have additional defects unrelated to sugar-phosphate toxicity. The *manA* and *rhaD* mutants were attenuated in the presence of sugar in the water, but not in its absence. The *galT* and *glpD* mutants were not attenuated under either condition. We used both male and female mice and observed no differences based on sex for any mutant, with the exception of *manA* with mannose ($P = 0.032$). We did not investigate the difference with *manA* further.

Resistance to sugar-phosphate toxicity can be obtained by mutation of a gene that encodes an enzyme required to generate the sugar-phosphate. These mutations also prevent successful utilization of the sugar as a nutrient but do not allow the accumulation of a sugar-phosphate intermediate (Fig. 3). Thus, some sugar utilization mutants are resistant to sugar-phosphate toxicity. From a therapeutics perspective, it would be ideal if these resistant mutants were also attenuated. To determine if this is the case in mice, we tested mutants deficient in *rhaB*, *mtlA*, and *araB* against wild type in the streptomycin-treated Swiss Webster mouse model, as described above. We included the appropriate sugar in the drinking water for each mutant. All three mutants were attenuated, but the attenuation was less severe than that observed with the corresponding sugar-phosphate mutants (*rhaD*, *mtlD*, and *araD*) (Fig. 5). This suggests that utilization alone contributes to fitness and that resistance to sugar-phosphate toxicity has a fitness cost.

Phylogenetic analysis of bacterial groups that may be susceptible to different sugar-phosphate toxicities. To determine which bacteria may be susceptible to the sugar-phosphate toxicities discussed in this report, we searched bacterial genomes for

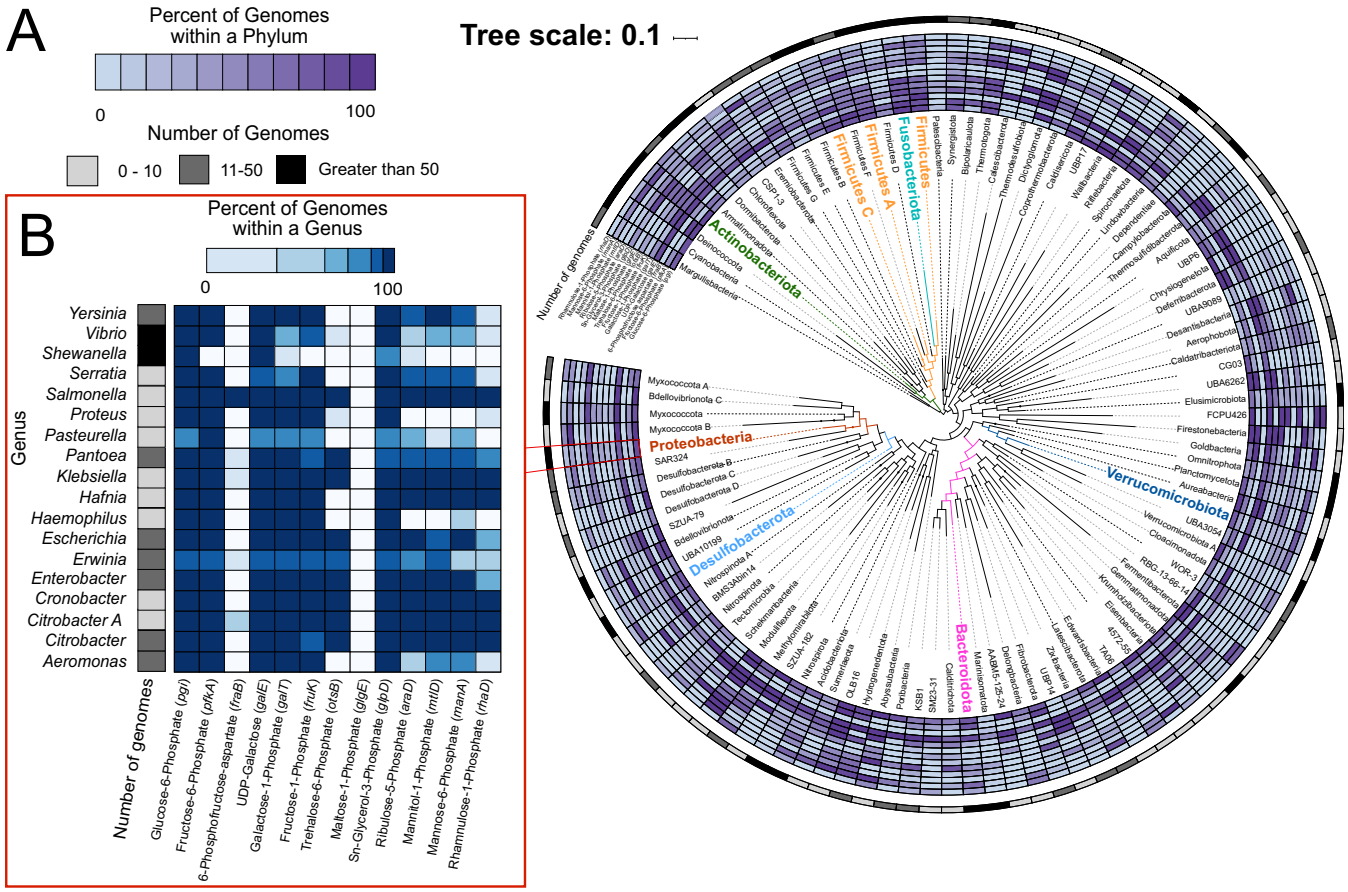

FIG 6 The taxonomic distribution of 13 genes that may cause sugar-phosphate toxicities when mutated. (A) The distribution of 13 genes that may cause sugar-phosphate toxicity determined from 30,238 bacterial genomes in the Genome Taxonomy Database using the AnnoTree software tool. Each purple-shaded tree ring quantifies the percentage of genomes in a phylum that contain the gene of interest. Phyla in which all genomes lacked homologs of all sugar phosphate genes are not shown. The gene of interest is labeled adjacent to the tree ring, along with the sugar-phosphate that may accumulate when the gene is mutated. Colored text denotes phyla that are dominant in the human gut. The outermost, gray-shaded ring represents the number of genomes analyzed for each phylum. (B) The blue heatmap shows the distribution of genes that, when mutated, may cause a sugar-phosphate toxicity in selected genera within the family *Enterobacteriaceae*. The far-left column depicts the number of genomes analyzed for each genus using the same gray scale as in panel A above. Table S1 in the supplemental material includes the data used to generate the heatmaps in panels A and B.

genes associated with each sugar-phosphate toxicity. The percentage of genomes within each bacterial phylum (Fig. 6A) or genus within the *Enterobacteriaceae* family (Fig. 6B) was plotted using AnnoTree software. The *galE* gene of the galactose pathway and two genes within the glycolytic pathway, *pgi* and *pfkA*, are very common, and it would be difficult to design narrow-spectrum therapeutics targeting the enzymes that these genes encode. In contrast, the *fraB* gene is extremely rare except in the *Firmicutes* and in the genus *Salmonella*, as has been previously reported (31). Three genes, *mtlD*, *araD*, and *rhaD*, were uncommon in most phyla but abundant in certain genera of the *Enterobacteriaceae* family, including *Salmonella*, *Escherichia*, *Enterobacter*, *Citrobacter*, *Klebsiella*, *Serratia*, and *Hafnia*. Thus, from a phylogenetics perspective, the enzymes that these three genes encode are good candidates for narrow-spectrum targets for some members of the carbapenem-resistant *Enterobacteriaceae*.

DISCUSSION

In previous work, we characterized the fructose-asparagine (F-Asn) utilization pathway of *Salmonella*, shown in Fig. 1 (30, 32). This pathway includes a phosphorylated intermediate, 6-P-F-Asp, that is converted by the FraB deglycase to glucose-6-phosphate and aspartate, which then enter central metabolism. When a *fraB* mutant is grown with F-Asn in the medium, 6-P-F-Asp accumulates and cell growth is inhibited (30) (Fig. 4). Mutants lacking *fraB* are highly attenuated in mouse models (30, 32). Since F-Asn is

available in mouse chow and in many human foods, it is possible that small-molecule inhibitors of FraB could represent a novel therapeutic for *Salmonella*-mediated gastroenteritis (34). Inhibitors of FraB would be narrow spectrum as it appears that the F-Asn utilization genes were acquired horizontally by *Salmonella* (or an earlier ancestor) from the *Firmicutes* (31). Besides some *Firmicutes*, only the *Salmonella* and a few *Klebsiella* and *Citrobacter* species can utilize F-Asn (Fig. 6) (31). The discovery of 6-P-F-Asp motivated us to search the literature for other examples, which we reviewed recently (3). We found descriptions of growth inhibition caused by the accumulation of sugar-phosphates dating back to the 1950s (37–39). In this work, we assembled a collection of mutants in *Salmonella* that might suffer sugar-phosphate toxicity and tested them for sugar-dependent growth inhibition *in vitro*. Following *in vitro* characterization, these mutants were studied in mouse models of infection to determine if inducing a sugar-phosphate toxicity might be effective therapeutically.

Our findings suggest that a *glpD* mutant does not suffer any detectable sugar-phosphate toxicity, as defined by an inhibition of growth in the presence of glycerol. A *manA* mutant suffers a moderate inhibition of growth in M9 minimal medium containing mannose (and no inhibition in LB containing mannose). However, *galE*, *galT*, *rhaD*, *mtlD*, and *araD* mutants all suffer severe sugar-phosphate toxicity, although the severity differs between medium types (Fig. 2). For example, the *rhaD* mutant appears to be more inhibited in LB than in M9, while the *araD* and *mtlD* mutants are more inhibited in M9 than in LB.

Mass spectrometry has been used to demonstrate that UDP-galactose and galactose-1-phosphate (Gal-1P) accumulate in an *Escherichia coli galE* mutant, while Gal-1P accumulates in an *E. coli galT* mutant (40). Additionally, Ru-5P has been shown to accumulate in *E. coli* (37), and Mtl-1P and 6-P-F-Asp have been shown to accumulate in *Salmonella* (30, 41). Here, we confirmed some of these findings. We demonstrated significant accumulation of Mtl-1P, Ru-5P, and 6-P-F-Asp in the *mtlD*, *araD*, and *fraB* mutants, respectively, compared to wild type (Fig. 4). Unfortunately, we were not able to measure rhamnulose-1-phosphate (Rhu-1P) in a *rhaD* mutant, as Rhu-1P is not available commercially to use as a standard. Synthesis of Rhu-1P, either chemically or enzymatically, is needed.

To determine if sugar-phosphate toxicities might cause decreased fitness during infection, we competed each sugar-phosphate mutant against wild type in a mouse model of gastroenteritis. Consistent with our *in vitro* data, the *glpD* mutant was not attenuated in our mouse model regardless of glycerol in the drinking water (Fig. 5). The *manA* mutant was attenuated but only when mannose was provided (Fig. 5). The *galT* mutant, which did display sugar-phosphate toxicity *in vitro*, is not attenuated in mice (Fig. 5). This finding is somewhat surprising as the accumulation of Gal-1P is known to lead to nucleotide imbalances and growth inhibition in *E. coli* (40, 42). Inhibition of this mutant by galactose *in vitro* but not during infection is intriguing. Mutants lacking *galE* are known to be attenuated in mice (43). Here, we confirm this as the *galE* mutant was extremely attenuated, regardless of the presence of galactose in the drinking water. However, it is well known that *galE* mutants of *Salmonella*, in the absence of galactose, fail to synthesize a complete lipopolysaccharide (LPS) structure which would reduce the mutant's fitness. However, interestingly, they do obtain enough galactose during infection to elaborate enough full-length LPS to generate an immune response to that LPS (43, 44). In our mouse studies, the attenuation of a *galE* mutant without galactose may be a result of this deficient LPS rather than sugar-phosphate toxicity. When galactose is provided, the *galE* mutant may be able to elaborate a more complete LPS, potentially recovering its fitness, but at the expense of sugar-phosphate toxicity being induced and thus again limiting survival. Regardless, GalE is unlikely to make a good therapeutic target as the bacterial enzyme has high structural conservation with human GALE (3).

Based on the data presented here, we believe that RhaD, MtlD, and AraD represent the most promising antimicrobial targets. Mutants lacking these genes are extremely

attenuated in mice when the appropriate sugar is included in the drinking water (Fig. 5). Interestingly, however, the mutants behave differently when sugar is not provided: the *rhaD* mutant is not attenuated, the *araD* mutant is moderately attenuated, and the *mtlD* mutant is extremely attenuated. These results may represent the relative quantities of these sugars available to *Salmonella* in the gut. Alternatively, the *araD* and *mtlD* mutants may have defects beyond sugar-phosphate toxicity that contribute to their attenuation. Consistent with the latter hypothesis, mannitol is a known osmoprotectant and it is likely that the *mtlD* mutant experiences osmolarity dysregulation in addition to sugar-phosphate toxicity (45, 46). The *araD* mutant is also susceptible to lysis, but only in the presence of arabinose (47). Overall, the profound effect of some sugars in the drinking water suggests that these sugars are not normally available to *Salmonella* in the gastrointestinal tract in quantities sufficient to intoxicate the mutants and that provision of the appropriate sugar in drinking water can overcome this deficiency.

The molecular mechanisms by which these sugar-phosphates are toxic are largely unknown, and much more research is needed in this area (3). As with any novel drug target, resistance mechanisms also need to be considered. For sugar-phosphate toxicity, resistance can arise from mutation of genes encoding enzymes required for the formation of the sugar-phosphate. However, these mutants are also sugar utilization mutants and may themselves have decreased fitness. We tested this hypothesis by assessing the phenotypes of an *rhaB*, an *araB*, and an *mtlA* mutant in mice. All three mutants were moderately attenuated (Fig. 5), indicating that acquiring resistance to sugar-phosphate toxicity also reduces fitness. This finding shows that at least part of the phenotype of *rhaD*, *araD*, and *mtlD* mutants in mice is due to a lack of sugar acquisition rather than sugar-phosphate toxicity.

While our study was performed in the clinically significant pathogen *Salmonella enterica* serovar Typhimurium, we thought it important to determine how widespread RhaD, AraD, and MtlD are in bacteria to consider the specificity of targeting these enzymes. Using bioinformatics, we found that all three are uncommon among most bacteria but are highly prevalent among *Cronobacter* and some of the genera making up the CRE and ESKAPE (*Enterococcus faecium*, *Staphylococcus aureus*, *Klebsiella pneumoniae*, *Acinetobacter baumannii*, *Pseudomonas aeruginosa*, and *Enterobacter* species) pathogens, including *Escherichia*, *Klebsiella*, *Serratia*, and *Enterobacter* (Fig. 6). Some of these organisms, especially *Escherichia* and *Klebsiella*, are associated with irritable bowel disease (IBD) (48–52). *Cronobacter* contaminates powdered baby formula and can cause fatal infections in infants (53). If inhibitors of these enzymes were to be developed, they could be used in combination with the appropriate sugar to reduce the abundance of these organisms in the gut (MtlD inhibitors may not require sugar). Beyond eliminating organisms, an interesting application of sugar-phosphate toxicity could be to "edit" the microbiome. For example, some strains of *Enterobacteriaceae* carry the *pks* island that encodes colibactin, which is associated with colon cancer (54–56). Inhibitors of RhaD, AraD, and/or MtlD could be used to remove these organisms from the gastrointestinal tract without causing disruption of the microbiota. The niche could then be filled with appropriate probiotic strains from the same genus that do not carry the *pks* island. Overall, it is likely that most pathogenic bacteria and fungi encode a metabolic pathway that could be targeted in this manner.

MATERIALS AND METHODS

Strains and media. Strains used in this study are listed in Table 1. Bacteria were routinely grown in lysogeny broth (LB) or on LB agar plates made by adding 1.5% (wt/vol) agar to LB broth (Fisher BioReagents). M9 minimal medium contained 1× M9 salts, 2 mM $MgSO_4$, 0.1 mM $CaCl_2$, 0.01 mM thiamine, and trace elements (57–59).

Construction of mutants. All *Salmonella* mutants predicted to undergo sugar-phosphate toxicity, except for *araD*, have been previously created using lambda Red mutagenesis in the Andrews-Polymenis and McClelland mutant library obtained from BEI Resources (60). Each gene in this collection has been disrupted by deleting all but the first 10 codons and the last 10 codons and inserting a gene encoding either chloramphenicol or kanamycin resistance that was cloned from pCLF3 (Cam^r) and pCLF4 (Kan^r) plasmids, respectively. The *araD* mutants and *pagC6*::Kan mutant were constructed using lambda Red mutagenesis in our laboratory (61). Briefly, the antibiotic resistance cassette of either pKD3

TABLE 1 Wild-type and isogenic sugar-phosphate mutant strains and plasmids

Strain or plasmid	Genotype or description	Source, construction, or reference
Strains		
ATCC 14028 (14028)	Wild-type *Salmonella enterica* subspecies *enterica* serovar Typhimurium	American Type Culture Collection (ATCC)
EFC008	14028 *galE1*::Cam	Original mutation from reference 60 transduced into 14028
EFB038	14028 *galE1*::Kan	Original mutation from reference 60 transduced into 14028
EFB001	14028 Δ*galE1*	Antibiotic cassette in EFC008 was removed using Flp recombinase encoded on pCP20 (61)
EFB053	14028 Δ*galE1* IG(*pagC*-STM14_1502)*6*::Kan	Transduction of IG(*pagC*-STM14_1502)*6*::Kan from EFB026 into EFB001
EFC009	14028 *galT1*::Cam	Original mutation from reference 60 transduced into 14028
EFB039	14028 *galT1*::Kan	Original mutation from reference 60 transduced into 14028
EFB002	14028 Δ*galT1*	Antibiotic cassette in EFC009 was removed using Flp recombinase encoded on pCP20 (61)
EFB054	14028 Δ*galT1* IG(*pagC*-STM14_1502)*6*::Kan	Transduction of IG(*pagC*-STM14_1502)*6*::Kan from EFB026 into EFB002
EFC015	14028 *rhaD1*::Cam	Original mutation from reference 60 transduced into 14028
EFB040	14028 *rhaD1*::Kan	Original mutation from reference 60 transduced into 14028
EFB003	14028 Δ*rhaD1*	Antibiotic cassette in EFC015 was removed using Flp recombinase encoded on pCP20 (61)
EFB055	14028 Δ*rhaD1* IG(*pagC*-STM14_1502)*6*::Kan	Transduction of IG(*pagC*-STM14_1502)*6*::Kan from EFB026 into EFB003
EFB006	14028 *glpD1*::Cam	Original mutation from reference 60 transduced into 14028
EFB041	14028 *glpD1*::Kan	Original mutation from reference 60 transduced into 14028
EFB009	14028 Δ*glpD1*	Antibiotic cassette in EFB041 was removed using Flp recombinase encoded on pCP20 (61)
EFB056	14028 Δ*glpD1* IG(*pagC*-STM14_1502)*6*::Kan	Transduction of IG(*pagC*-STM14_1502)*6*::Kan from EFB026 into EFB009
EFC019	14028 *mtlD1*::Cam	Original mutation from reference 60 transduced into 14028
EFB042	14028 *mtlD1*::Kan	Original mutation from reference 60 transduced into 14028
EFB004	14028 Δ*mtlD1*	Antibiotic cassette in EFC019 was removed using Flp recombinase encoded on pCP20 (61)
EFB057	14028 Δ*mtlD1* IG(*pagC*-STM14_1502)*6*::Kan	Transduction of IG(*pagC*-STM14_1502)*6*::Kan from EFB026 into EFB004
EFC021	14028 *manA1*::Cam	Original mutation from reference 60 transduced into 14028
EFB005	14028 Δ*manA1*	Antibiotic cassette in EFC021 was removed using Flp recombinase encoded on pCP20 (61)
EFB058	14028 Δ*manA1* IG(*pagC*-STM14_1502)*6*::Kan	Transduction of IG(*pagC*-STM14_1502)*6*::Kan from EFB026 into EFB005
EFC037	14028 *araD6*::Kan	Lambda Red mutation of *araD* made using PCR primers BA3522 and BA3523 to amplify the Kan^r gene from pKD4. The resulting mutation was then transduced into 14028.
EFC039	14028 *araD6*::Cam	Lambda Red mutation of *araD* made using PCR primers BA3522 and BA3523 to amplify the Cam^r gene from pKD3. The resulting mutation was then transduced into 14028.
HMB206	14028 *fraB80*::Kan	30
JLD1214	14028 IG(*pagC*-STM14_1502)::Cam	32
EFB026	14028 IG(*pagC*-STM14_1502)*6*::Kan	Lambda Red mutation downstream of *pagC* made using PCR primers BA3849 and BA3850 to amplify the Kan^r gene from pKD4
EFB051	14028 IG(*pagC*-STM14_1502)*6*::Kan	Transduction of IG(*pagC*-STM14_1502)*6*::Kan from EFB026 into 14028
EFB063	14028 *rhaB1*::Kan	Original mutation from reference 60 transduced into 14028
EFB037	14028 *araB1*::Cam	Original mutation from reference 60 transduced into 14028
EFB036	14028 *mtlA1*::Cam	Original mutation from reference 60 transduced into 14028
Plasmids		
pKD46	PBAD *gam bet exo* pSC101 *oriTS* (Amp^r)	61
pKD3	FRT[a]-*cam*-FRT *oriR6K* (Amp^r)	61
pKD4	FRT-*kan*-FRT *oriR6K* (Amp^r)	61
pCP20	cI857 λPR *flp* pSC101 *oriTS* (Amp^r Cam^r)	68

[a]FRT, FLP recombination target.

(Cam^r) or pKD4 (Kan^r) was amplified with PCR using primers that bind the P1 and P2 regions of the template plasmids, with an additional 40-nucleotide tail on each primer representing the desired insertion site in the chromosome. Primer sequences used are listed in Table 2. The resulting PCR product was electroporated into strain 14028 carrying pKD46, and recombinants were selected on LB plus antibiotic at 37°C. The insertion was confirmed using PCR with one primer inside the antibiotic resistance gene and the other outside the region of recombination. Each allele of interest was transduced using phage P22 HT *int* (62) into our laboratory strain of 14028. Insertions of antibiotic resistance genes that had been constructed using lambda Red mutagenesis were subsequently deleted using the Flp recombinase encoded on a temperature-sensitive plasmid, pCP20 (61). This plasmid was electroporated into mutants

TABLE 2 PCR primers

Primer	Sequence	Description
BA3522	GGAGAAAACAATGTTAGAAGATCTCAAACGCCAGGTACTGGTGTAGGCTGGAGCTGCTTC	Forward primer for *araD* lambda Red mutagenesis
BA3523	TTTAGAGGCATTACTGCCCGTAATAGGCTTTTGCGCCGTGCATATGAATATCCTCCTTAG	Reverse primer for *araD* lambda Red mutagenesis
BA3849	CGAAGGCGGTCACAAAATCTTGATGACATTGTGATTAATGTGTAGGCTGGAGCTGCTTCG	Forward primer for *pagC* intergenic region lambda Red mutagenesis
BA3850	CTTCTTTACCAGTGACACGTACCTGCCTGTCTTTTCTCTCATATGAATATCCTCCTTAG	Reverse primer for *pagC* intergenic region lambda Red mutagenesis

of interest by selection on LB-ampicillin (LB-Amp) at 30°C. Single colonies were streaked onto LB and incubated at 42°C to allow for loss of the antibiotic cassette and curing of the plasmid. Individual colonies were confirmed to lack the antibiotic resistance gene and pCP20 by patching on LB-Amp (pCP20) and LB-Kan or LB-Cam. PCR was used to verify the deletions.

Growth assays. Growth of strains was assessed using clear, flat-bottom, 96-well plates. Bacterial cultures that had been grown overnight were centrifuged at 18,000 $\times$ *g* and resuspended in an equal volume of sterile water. Two microliters of bacteria was then inoculated into a well containing 198 μL of the indicated medium. A Breathe-Easy membrane film (Diversified Biotech) was placed over the 96-well plate. Growth was measured using a SpectraMax M5 (Molecular Devices) microplate reader and the SoftMax Pro 6.1 software, taking hourly readings of optical density at 600 nm (OD_{600}) over a course of 17 to 20 h at 37°C.

Quantitative mass spectrometry for sugar-phosphates. Cell pellets for mass spectrometry (MS) were prepared by inoculating 5 mL of LB containing the indicated sugar at 5 mM with 50 μL of overnight culture in a glass tube and incubating at 37°C for 4 h. After 4 h, the entire culture was poured into a 15-mL conical tube and centrifuged for 10 min at 10,000 $\times$ *g* at 4°C. The majority of the supernatant was poured off, leaving about 1 mL in which to resuspend the pellet and transfer it to a 1.5-mL microcentrifuge tube. The bacteria were centrifuged for 1 min at 18,000 $\times$ *g*. All supernatant was pipetted off, and cell pellet was immediately frozen at −80°C. For each measurement, 100 μL of *Salmonella* cell pellets (equivalent to 5-mL samples of cells) was used. Two hundred microliters of liquid chromatography (LC)-grade water was added to result in a final volume of 300 μL, which was split into three aliquots for subsequent use as analytical replicates for each analysis. The sugar-phosphate was extracted from each 100-μL aliquot, by adding 250 μL of chilled LC-grade water and 500 μL of chilled methanol (Fisher Optima LC/MS grade; Fisher Scientific) with 20 nmol [^{13}C]fructose-asparagine ([^{13}C]F-Asn) added as internal standard. [^{13}C]F-Asn was used as internal standard due to the lower cost and simplicity of the synthesis of [^{13}C]F-Asn compared to the ^{13}C heavy atom-labeled sugar-phosphates. The cell suspension was then vortexed for 2 min to facilitate pellet disruption and metabolite extraction. Samples were subjected to 10 cycles of ultrasonication (30 s each with 30-s intervals in between) using a Bioruptor Pico (Diagenode). Following cell lysis, samples were centrifuged at 16,000 $\times$ *g* for 15 min at 4°C, and the supernatants were transferred to new tubes and dried under vacuum (SpeedVac concentrator; Thermo Scientific). Before mass spectrometry analysis, the dried pellets were resuspended in 50 μL water-acetonitrile, 98%:2%, with 0.1% (vol/vol) formic acid (LC-MS grade; Thermo Scientific) and filtered using a 0.2-μm polytetrafluoroethylene (PTFE) filter (Thermo Scientific). The supernatant of the flowthrough fraction was then injected for liquid chromatographic-mass spectrometric analysis. For the standard curve analysis, different amounts of standard sugar-phosphates (0, 20, 80, 160, 200, 400, or 600 nmol) were spiked into the extraction solvent and were prepared as described above. Ten microliters of each sample was introduced into an Ultimate 3000 ultraperformance LC (Thermo Scientific) system with an HSS T3, C_{18} column (Waters; 2.1 μm by 100 mm, 1.8 μm) and coupled into a triple quadrupole mass spectrometer (Thermo Quantiva TQ-S). Mobile phases were buffer A, 0.1% (vol/vol) formic acid (LC-MS grade; Thermo Scientific) in water, and buffer B, 0.1% (vol/vol) formic acid in acetonitrile. A gradient separation started with 2% B for 3 min at a flow rate of 100 μL/min and was then followed by a gradient: 3 to 4 min, 2 to 10% B; 4 to 7 min, 10 to 98% B; 7 to 7.5 min, 98% B; 7.5 to 7.6 min, 98 to 2% B; 7.6 to 10 min, 2% B. The mass spectrometer was operated in positive-ion electrospray ionization mode (ESI+) with a capillary voltage at 4 kV, source temperature of 100°C, desolvation temperature of 350°C, sheath gas flow of 12 L/min, and auxiliary gas flow of 13 L/min. The gas flow rate for the collision cell was 0.15 mL/min. A multiple-reaction monitoring (MRM) mode was used for sugar phosphate analysis. Skyline (v20.2; MacCoss Lab, Department of Genome Sciences, University of Washington, Seattle, WA, USA) was used for calculating the peak area of each transition. Transition conditions, including retention time, precursor ion, product ion, and collision energy, are described in Fig. 4B.

Animal experiments. The fitness of *Salmonella* mutants was compared to that of the wild type in the streptomycin-treated Swiss Webster mouse model (30). The mice were treated by oral gavage with 20 mg of streptomycin (35). Twenty-four hours later, the mice were inoculated with a 1:1 ratio of wild-type and mutant bacteria. The inoculum titer was determined on LB-Kan and LB-Cam to determine the input quantities of the two strains being used. Total inoculum dose was 1 $\times$ 10^7 CFU. Where indicated, mice were provided the sugar of interest in their drinking water (100 mM). At 4 days postinfection, mice were euthanized and each cecum was harvested. Cecum samples were weighed, homogenized, and dilution plated on LB-Kan and LB-Cam for enumeration of CFU.

Phylogenetic and genomic analyses. With the exception of genes related to fructose-asparagine, the genes described below that, when mutated, result in toxic sugar-phosphate intermediates were searched in the AnnoTree v1.2 database with default parameters (e−5). These genes, the sugar-phosphate that accumulates, and the enzyme EC number were as follows: *pgi* (glucose-6-phosphate; EC 5.3.1.9), *pfkA* (fructose-6-phosphate; EC 2.7.1.11), *fraB* (6-phosphofructose aspartate; accession no. WP_010989080.1), *galE* (UDP-galactose; EC 5.1.3.2), *galT* (galactose-1-phosphate; EC 2.7.7.12), *fruK* (fructose-1-phosphate; EC 2.7.1.56), *otsB* (trehalose-6-phosphate; EC 3.1.3.12), *glgE* (maltose-1-phosphate; EC 2.4.99.16), *glpD* (*sn*-glycerol-3-phosphate; EC 1.1.5.3), *araD* (ribulose-5-phosphate; EC 5.1.3.4), *manA* (mannose-6-phosphate; EC 5.3.1.8), and *rhaD* (rhamnulose-1-phosphate; EC 4.1.2.19). For *fraB* (6-phosphofructose aspartate), we used previously determined cutoffs (BLAST e−20) to differentiate homologs from fructoselysine-6-P-deglycase (*frlB*) (31, 63). The AnnoTree v1.2 database was downloaded and analyzed on 18 February 2021 (http://annotree.uwaterloo.ca/app/downloads.html) (63). The maximum likelihood phylum tree was downloaded from AnnoTree v1.2, with methods for tree generation detailed in reference 64. Briefly, this phylogenetic tree was constructed using 120 ubiquitous single-copy marker genes (bac120 marker set) from 30,238 bacterial genomes that were obtained from GTDB r95. The relative abundance of genes in the genomes for each phylum was overlaid onto the phylogenetic tree and visualized in iTOL 5.7 (65). For selected gut-relevant genera within the *Enterobacteriaceae*, the percentage of the sugar genes in genomes from each genus was calculated. The number of genomes in the genus is derived from the parameters that are used for searches in the AnnoTree v1.2 database (63). The heatmap was created using RStudio and visualized using Adobe Illustrator (66).

Animal assurance. All animal work was performed using protocols approved by our Institutional Animal Care and Use Committee (IACUC; OSU 2009A0035) and in accordance with the relevant guidelines set forth in the *Guide for the Care and Use of Laboratory Animals* (67).

SUPPLEMENTAL MATERIAL

Supplemental material is available online only.

SUPPLEMENTAL FILE 1, XLSX file, 0.02 MB.

ACKNOWLEDGMENTS

We acknowledge support from the NIH (R01AI140541 to B.M.M.A., R01AI143288 and R01AI116119 to K.C.W., V.H.W., and B.M.M.A.; T32GM068412 and T32AI165391 to E.F.B.). This content is solely the responsibility of the authors and does not necessarily represent the official views of the funding agencies.

We are grateful for helpful discussions and input from the labs of Venkat Gopalan, Ned Behrman, Mark Mitton-Fry, Charles Bell, and Steffen Lindert (OSU).

REFERENCES

1. Ribeiro da Cunha B, Fonseca LP, Calado CRC. 2019. Antibiotic discovery: where have we come from, where do we go? Antibiotics (Basel) 8:45. https://doi.org/10.3390/antibiotics8020045.
2. World Health Organization. 2017. Prioritization of pathogens to guide discovery, research and development of new antibiotics for drug-resistant bacterial infections, including tuberculosis. WHO/EMP/IAU/2017.12. World Health Organization, Geneva, Switzerland.
3. Boulanger EF, Sabag-Daigle A, Thirugnanasambantham P, Gopalan V, Ahmer BMM. 2021. Sugar-phosphate toxicities. Microbiol Mol Biol Rev 85:e0012321. https://doi.org/10.1128/MMBR.00123-21.
4. CDC. 2019. Antibiotic resistance threats in the United States. CDC, Atlanta, GA.
5. Grimont PAD, Weill F-X. 2007. Antigenic formulae of the Salmonella serovars, 9th ed, p 166. WHO Collaborating Centre for Reference and Research on Salmonella, Institut Pasteur, Paris, France.
6. Pearce ME, Langridge GC, Lauer AC, Grant K, Maiden MCJ, Chattaway MA. 2021. An evaluation of the species and subspecies of the genus *Salmonella* with whole genome sequence data: proposal of type strains and epithets for novel *S. enterica* subspecies VII, VIII, IX, X and XI. Genomics 113:3152–3162. https://doi.org/10.1016/j.ygeno.2021.07.003.
7. Scallan E, Hoekstra RM, Angulo FJ, Tauxe RV, Widdowson M-A, Roy SL, Jones JL, Griffin PM. 2011. Foodborne illness acquired in the United States–major pathogens. Emerg Infect Dis 17:7–15. https://doi.org/10.3201/eid1701.P11101.
8. Kirk MD, Pires SM, Black RE, Caipo M, Crump JA, Devleesschauwer B, Döpfer D, Fazil A, Fischer-Walker CL, Hald T, Hall AJ, Keddy KH, Lake RJ, Lanata CF, Torgerson PR, Havelaar AH, Angulo FJ. 2015. World Health Organization estimates of the global and regional disease burden of 22 foodborne bacterial, protozoal, and viral diseases, 2010: a data synthesis. PLoS Med 12:e1001921. https://doi.org/10.1371/journal.pmed.1001921.
9. Dewey-Mattia D, Manikonda K, Hall AJ, Wise ME, Crowe SJ. 2018. Surveillance for foodborne disease outbreaks - United States, 2009–2015. MMWR Surveill Summ 67:1–11. https://doi.org/10.15585/mmwr.ss6710a1.
10. Aserkoff B, Bennett JV. 1969. Effect of antibiotic therapy in acute salmonellosis on the fecal excretion of salmonellae. N Engl J Med 281:636–640. https://doi.org/10.1056/NEJM196909182811202.
11. Nelson JD, Kusmiesz H, Jackson LH, Woodman E. 1980. Treatment of *Salmonella* gastroenteritis with ampicillin, amoxicillin, or placebo. Pediatrics 65:1125–1130. https://doi.org/10.1542/peds.65.6.1125.
12. Onwuezobe IA, Oshun PO, Odigwe CC. 2012. Antimicrobials for treating symptomatic non-typhoidal *Salmonella* infection. Cochrane Database Syst Rev 11:CD001167. https://doi.org/10.1002/14651858.CD001167.pub2.
13. Wistrom J, Jertborn M, Ekwall E, Norlin K, Söderquist B, Strömberg A, Lundholm R, Hogevik H, Lagergren L, Englund G, Norrby SR. 1992. Empiric treatment of acute diarrheal disease with norfloxacin. A randomized, placebo-controlled study. Swedish Study Group. Ann Intern Med 117:202–208. https://doi.org/10.7326/0003-4819-117-3-202.
14. Dolowschiak T, Mueller AA, Pisan LJ, Feigelman R, Felmy B, Sellin ME, Namineni S, Nguyen BD, Wotzka SY, Heikenwalder M, von Mering C, Mueller C, Hardt W-D. 2016. IFN-gamma hinders recovery from mucosal inflammation during antibiotic therapy for *Salmonella* gut infection. Cell Host Microbe 20:238–249. https://doi.org/10.1016/j.chom.2016.06.008.
15. Kotloff KL. 2022. Bacterial diarrhoea. Curr Opin Pediatr 34:147–155. https://doi.org/10.1097/MOP.0000000000001107.
16. Ohl ME, Miller SI. 2001. *Salmonella*: a model for bacterial pathogenesis. Annu Rev Med 52:259–274. https://doi.org/10.1146/annurev.med.52.1.259.

17. Galan JE. 2021. *Salmonella* Typhimurium and inflammation: a pathogen-centric affair. Nat Rev Microbiol 19:716–725. https://doi.org/10.1038/s41579-021-00561-4.
18. Fattinger SA, Sellin ME, Hardt WD. 2021. *Salmonella* effector driven invasion of the gut epithelium: breaking in and setting the house on fire. Curr Opin Microbiol 64:9–18. https://doi.org/10.1016/j.mib.2021.08.007.
19. Rivera-Chavez F, Baumler AJ. 2015. The pyromaniac inside you: Salmonella metabolism in the host gut. Annu Rev Microbiol 69:31–48. https://doi.org/10.1146/annurev-micro-091014-104108.
20. Grassl GA, Finlay BB. 2008. Pathogenesis of enteric Salmonella infections. Curr Opin Gastroenterol 24:22–26. https://doi.org/10.1097/MOG.0b013e3282f21388.
21. Bevins CL, Salzman NH. 2011. The potter's wheel: the host's role in sculpting its microbiota. Cell Mol Life Sci 68:3675–3685. https://doi.org/10.1007/s00018-011-0830-3.
22. Borton MA, Sabag-Daigle A, Wu J, Solden LM, O'Banion BS, Daly RA, Wolfe RA, Gonzalez JF, Wysocki VH, Ahmer BMM, Wrighton KC. 2017. Chemical and pathogen-induced inflammation disrupt the murine intestinal microbiome. Microbiome 5:47. https://doi.org/10.1186/s40168-017-0264-8.
23. Thiennimitr P, Winter SE, Winter MG, Xavier MN, Tolstikov V, Huseby DL, Sterzenbach T, Tsolis RM, Roth JR, Bäumler AJ. 2011. Intestinal inflammation allows Salmonella to use ethanolamine to compete with the microbiota. Proc Natl Acad Sci U S A 108:17480–17485. https://doi.org/10.1073/pnas.1107857108.
24. Rogers AWL, Tsolis RM, Baumler AJ. 2021. Salmonella versus the microbiome. Microbiol Mol Biol Rev 85:e00027-19. https://doi.org/10.1128/MMBR.00027-19.
25. Maier L, Vyas R, Cordova CD, Lindsay H, Schmidt TSB, Brugiroux S, Periaswamy B, Bauer R, Sturm A, Schreiber F, von Mering C, Robinson MD, Stecher B, Hardt W-D. 2013. Microbiota-derived hydrogen fuels Salmonella typhimurium invasion of the gut ecosystem. Cell Host Microbe 14:641–651. https://doi.org/10.1016/j.chom.2013.11.002.
26. Lee JY, Tsolis RM, Baumler AJ. 2022. The microbiome and gut homeostasis. Science 377:eabp9960. https://doi.org/10.1126/science.abp9960.
27. Stecher B, Robbiani R, Walker AW, Westendorf AM, Barthel M, Kremer M, Chaffron S, Macpherson AJ, Buer J, Parkhill J, Dougan G, von Mering C, Hardt W-D. 2007. *Salmonella enterica* serovar Typhimurium exploits inflammation to compete with the intestinal microbiota. PLoS Biol 5:2177–2189. https://doi.org/10.1371/journal.pbio.0050244.
28. Rivera-Chavez F, Zhang LF, Faber F, Lopez CA, Byndloss MX, Olsan EE, Xu G, Velazquez EM, Lebrilla CB, Winter SE, Bäumler AJ. 2016. Depletion of butyrate-producing clostridia from the gut microbiota drives an aerobic luminal expansion of Salmonella. Cell Host Microbe 19:443–454. https://doi.org/10.1016/j.chom.2016.03.004.
29. Deatherage Kaiser BL, Li J, Sanford JA, Kim Y-M, Kronewitter SR, Jones MB, Peterson CT, Peterson SN, Frank BC, Purvine SO, Brown JN, Metz TO, Smith RD, Heffron F, Adkins JN. 2013. A multi-omic view of host-pathogen-commensal interplay in Salmonella-mediated intestinal infection. PLoS One 8:e67155. https://doi.org/10.1371/journal.pone.0067155.
30. Sabag-Daigle A, Blunk HM, Sengupta A, Wu J, Bogard AJ, Ali MM, Stahl C, Wysocki VH, Gopalan V, Behrman EJ, Ahmer BMM. 2016. A metabolic intermediate of the fructose-asparagine utilization pathway inhibits growth of a *Salmonella fraB* mutant. Sci Rep 6:28117. https://doi.org/10.1038/srep28117.
31. Sabag-Daigle A, Wu J, Borton MA, Sengupta A, Gopalan V, Wrighton KC, Wysocki VH, Ahmer BMM. 2018. Identification of bacterial species that can utilize fructose-asparagine. Appl Environ Microbiol 84:e01957-17. https://doi.org/10.1128/AEM.01957-17.
32. Ali MM, Newsom DL, González JF, Sabag-Daigle A, Stahl C, Steidley B, Dubena J, Dyszel JL, Smith JN, Dieye Y, Arsenescu R, Boyaka PN, Krakowka S, Romeo T, Behrman EJ, White P, Ahmer BMM. 2014. Fructose-asparagine is a primary nutrient during growth of Salmonella in the inflamed intestine. PLoS Pathog 10:e1004209. https://doi.org/10.1371/journal.ppat.1004209.
33. Wu J, Sabag-Daigle A, Borton MA, Kop LFM, Szkoda BE, Deatherage Kaiser BL, Lindemann SR, Renslow RS, Wei S, Nicora CD, Weitz KK, Kim Y-M, Adkins JN, Metz TO, Boyaka P, Gopalan V, Wrighton KC, Wysocki VH, Ahmer BMM. 2018. Salmonella-mediated inflammation eliminates competitors for fructose-asparagine in the gut. Infect Immun 86:e00945-17. https://doi.org/10.1128/IAI.00945-17.
34. Wu J, Sabag-Daigle A, Metz TO, Deatherage Kaiser BL, Gopalan V, Behrman EJ, Wysocki VH, Ahmer BMM. 2018. Measurement of fructose-asparagine concentrations in human and animal foods. J Agric Food Chem 66:212–217. https://doi.org/10.1021/acs.jafc.7b04237.
35. Barthel M, Hapfelmeier S, Quintanilla-Martínez L, Kremer M, Rohde M, Hogardt M, Pfeffer K, Rüssmann H, Hardt W-D. 2003. Pretreatment of mice with streptomycin provides a *Salmonella enterica* serovar Typhimurium colitis model that allows analysis of both pathogen and host. Infect Immun 71:2839–2858. https://doi.org/10.1128/IAI.71.5.2839-2858.2003.
36. Gunn JS, Ryan SS, Van Velkinburgh JC, Ernst RK, Miller SI. 2000. Genetic and functional analysis of a PmrA-PmrB-regulated locus necessary for lipopolysaccharide modification, antimicrobial peptide resistance, and oral virulence of *Salmonella enterica* serovar Typhimurium. Infect Immun 68:6139–6146. https://doi.org/10.1128/IAI.68.11.6139-6146.2000.
37. Englesberg E, Anderson RL, Weinberg R, Lee N, Hoffee P, Huttenhauer G, Boyer H. 1962. L-Arabinose-sensitive, L-ribulose 5-phosphate 4-epimerase-deficient mutants of *Escherichia coli*. J Bacteriol 84:137–146. https://doi.org/10.1128/jb.84.1.137-146.1962.
38. Fukasawa T, Nikaido H. 1959. Galactose-sensitive mutants of Salmonella. Nature 184(Suppl 15):1168–1169. https://doi.org/10.1038/1841168a0.
39. Kurahashi K, Wahba AJ. 1958. Interference with growth of certain *Escherichia coli* mutants by galactose. Biochim Biophys Acta 30:298–302. https://doi.org/10.1016/0006-3002(58)90054-4.
40. Barupal DK, Lee SJ, Karoly ED, Adhya S. 2013. Inactivation of metabolic genes causes short- and long-range dys-regulation in *Escherichia coli* metabolic network. PLoS One 8:e78360. https://doi.org/10.1371/journal.pone.0078360.
41. Jensen P, Parkes C, Berkowitz D. 1972. Mannitol sensitivity. J Bacteriol 111:351–355. https://doi.org/10.1128/jb.111.2.351-355.1972.
42. Lee SJ, Trostel A, Adhya S. 2014. Metabolite changes signal genetic regulatory mechanisms for robust cell behavior. mBio 5:e00972-13. https://doi.org/10.1128/mBio.00972-13.
43. Germanier R, Furer E. 1971. Immunity in experimental salmonellosis. II. Basis for the avirulence and protective capacity of *gal* E mutants of *Salmonella typhimurium*. Infect Immun 4:663–673. https://doi.org/10.1128/iai.4.6.663-673.1971.
44. Germanier R. 1970. Immunity in experimental salmonellosis I. Protection induced by rough mutants of *Salmonella typhimurium*. Infect Immun 2:309–315. https://doi.org/10.1128/iai.2.3.309-315.1970.
45. Solomon E, Lin EC. 1972. Mutations affecting the dissimilation of mannitol by *Escherichia coli* K-12. J Bacteriol 111:566–574. https://doi.org/10.1128/jb.111.2.566-574.1972.
46. Nguyen T, Kim T, Ta HM, Yeo WS, Choi J, Mizar P, Lee SS, Bae T, Chaurasia AK, Kim KK. 2019. Targeting mannitol metabolism as an alternative antimicrobial strategy based on the structure-function study of mannitol-1-phosphate dehydrogenase in *Staphylococcus aureus*. mBio 10:e02660-18. https://doi.org/10.1128/mBio.02660-18.
47. Tanaka T, Muroi H, Sunada C, Taniguchi M, Oi S. 1991. Determination of effector molecules in L-arabinose-induced bulge formation and lysis of *Escherichia coli* IFO 3545. J Gen Microbiol 137:1163–1169. https://doi.org/10.1099/00221287-137-5-1163.
48. Darfeuille-Michaud A, Neut C, Barnich N, Lederman E, Di Martino P, Desreumaux P, Gambiez L, Joly B, Cortot A, Colombel JF. 1998. Presence of adherent *Escherichia coli* strains in ileal mucosa of patients with Crohn's disease. Gastroenterology 115:1405–1413. https://doi.org/10.1016/s0016-5085(98)70019-8.
49. Federici S, Kredo-Russo S, Valdés-Mas R, Kviatcovsky D, Weinstock E, Matiuhin Y, Silberberg Y, Atarashi K, Furuichi M, Oka A, Liu B, Fibelman M, Weiner IN, Khabra E, Cullin N, Ben-Yishai N, Inbar D, Ben-David H, Nicenboim J, Kowalsman N, Lieb W, Kario E, Cohen T, Geffen YF, Zelcbuch L, Cohen A, Rappo U, Gahali-Sass I, Golembo M, Lev V, Dori-Bachash M, Shapiro H, Moresi C, Cuevas-Sierra A, Mohapatra G, Kern L, Zheng D, Nobs SP, Suez J, Stettner N, Harmelin A, Zak N, Puttagunta S, Bassan M, Honda K, Sokol H, Bang C, Franke A, Schramm C, Maharshak N, Sartor RB, Sorek R, Elinav E. 2022. Targeted suppression of human IBD-associated gut microbiota commensals by phage consortia for treatment of intestinal inflammation. Cell 185:2879–2898.e24. https://doi.org/10.1016/j.cell.2022.07.003.
50. Elhenawy W, Tsai CN, Coombes BK. 2019. Host-specific adaptive diversification of Crohn's disease-associated adherent-invasive *Escherichia coli*. Cell Host Microbe 25:301–312.e5. https://doi.org/10.1016/j.chom.2018.12.010.
51. Elhenawy W, Hordienko S, Gould S, Oberc AM, Tsai CN, Hubbard TP, Waldor MK, Coombes BK. 2021. High-throughput fitness screening and transcriptomics identify a role for a type IV secretion system in the pathogenesis of Crohn's disease-associated *Escherichia coli*. Nat Commun 12:2032. https://doi.org/10.1038/s41467-021-22306-w.
52. Kitamoto S, Nagao-Kitamoto H, Jiao Y, Gillilland MG, III, Hayashi A, Imai J, Sugihara K, Miyoshi M, Brazil JC, Kuffa P, Hill BD, Rizvi SM, Wen F, Bishu S, Inohara N, Eaton KA, Nusrat A, Lei YL, Giannobile WV, Kamada N. 2020. The intermucosal connection between the mouth and gut in commensal pathobiont-driven colitis. Cell 182:447–462.e14. https://doi.org/10.1016/j.cell.2020.05.048.
53. Norberg S, Stanton C, Ross RP, Hill C, Fitzgerald GF, Cotter PD. 2012. *Cronobacter* spp. in powdered infant formula. J Food Prot 75:607–620. https://doi.org/10.4315/0362-028X.JFP-11-285.

54. Arthur JC, Perez-Chanona E, Mühlbauer M, Tomkovich S, Uronis JM, Fan T-J, Campbell BJ, Abujamel T, Dogan B, Rogers AB, Rhodes JM, Stintzi A, Simpson KW, Hansen JJ, Keku TO, Fodor AA, Jobin C. 2012. Intestinal inflammation targets cancer-inducing activity of the microbiota. Science 338:120–123. https://doi.org/10.1126/science.1224820.
55. Strakova N, Korena K, Karpiskova R. 2021. *Klebsiella pneumoniae* producing bacterial toxin colibactin as a risk of colorectal cancer development - a systematic review. Toxicon 197:126–135. https://doi.org/10.1016/j.toxicon.2021.04.007.
56. Nougayrede JP, Homburg S, Taieb F, Boury M, Brzuszkiewicz E, Gottschalk G, Buchrieser C, Hacker J, Dobrindt U, Oswald E. 2006. *Escherichia coli* induces DNA double-strand breaks in eukaryotic cells. Science 313:848–851. https://doi.org/10.1126/science.1127059.
57. Griffith KL, Wolf RE, Jr. 2002. Measuring beta-galactosidase activity in bacteria: cell growth, permeabilization, and enzyme assays in 96-well arrays. Biochem Biophys Res Commun 290:397–402. https://doi.org/10.1006/bbrc.2001.6152.
58. Price-Carter M, Tingey J, Bobik TA, Roth JR. 2001. The alternative electron acceptor tetrathionate supports B12-dependent anaerobic growth of *Salmonella enterica* serovar Typhimurium on ethanolamine or 1,2-propanediol. J Bacteriol 183:2463–2475. https://doi.org/10.1128/JB.183.8.2463-2475.2001.
59. Nuccio SP, Baumler AJ. 2014. Comparative analysis of *Salmonella* genomes identifies a metabolic network for escalating growth in the inflamed gut. mBio 5:e00929-14. https://doi.org/10.1128/mBio.00929-14.
60. Santiviago CA, Reynolds MM, Porwollik S, Choi S-H, Long F, Andrews-Polymenis HL, McClelland M. 2009. Analysis of pools of targeted Salmonella deletion mutants identifies novel genes affecting fitness during competitive infection in mice. PLoS Pathog 5:e1000477. https://doi.org/10.1371/journal.ppat.1000477.
61. Datsenko KA, Wanner BL. 2000. One-step inactivation of chromosomal genes in *Escherichia coli* K-12 using PCR products. Proc Natl Acad Sci U S A 97:6640–6645. https://doi.org/10.1073/pnas.120163297.
62. Mahan MJ, Slauch JM, Mekalanos JJ. 1993. Bacteriophage P22 transduction of integrated plasmids: single-step cloning of *Salmonella typhimurium* gene fusions. J Bacteriol 175:7086–7091. https://doi.org/10.1128/jb.175.21.7086-7091.1993.
63. Mendler K, Chen H, Parks DH, Lobb B, Hug LA, Doxey AC. 2019. AnnoTree: visualization and exploration of a functionally annotated microbial tree of life. Nucleic Acids Res 47:4442–4448. https://doi.org/10.1093/nar/gkz246.
64. Parks DH, Chuvochina M, Waite DW, Rinke C, Skarshewski A, Chaumeil P-A, Hugenholtz P. 2018. A standardized bacterial taxonomy based on genome phylogeny substantially revises the tree of life. Nat Biotechnol 36:996–1004. https://doi.org/10.1038/nbt.4229.
65. Letunic I, Bork P. 2019. Interactive Tree Of Life (iTOL) v4: recent updates and new developments. Nucleic Acids Res 47:W256–W259. https://doi.org/10.1093/nar/gkz239.
66. RStudio Team. 2020. RStudio: integrated development for R. RStudio, Boston, MA. http://www.rstudio.com/.
67. National Research Council. 2011. Guide for the care and use of laboratory animals, 8th ed. National Academies Press, Washington, DC.
68. Cherepanov PP, Wackernagel W. 1995. Gene disruption in *Escherichia coli*: TcR and KmR cassettes with the option of Flp-catalyzed excision of the antibiotic-resistance determinant. Gene 158:9–14. https://doi.org/10.1016/0378-1119(95)00193-A.